

AD-A060 756

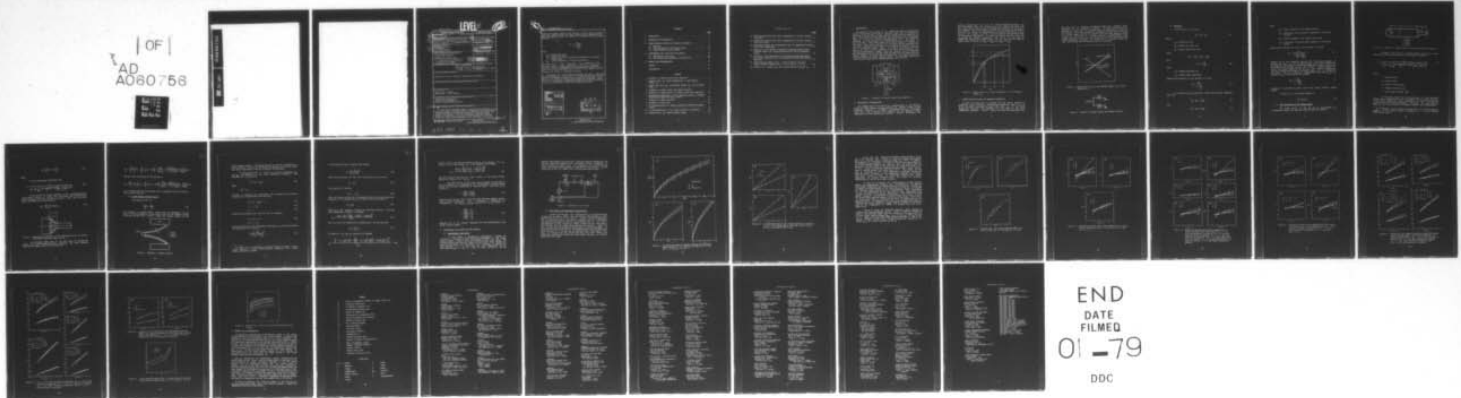
HARRY DIAMOND LABS ADELPHI MD
TEMPERATURE COMPENSATION OF LAMINAR PROPORTIONAL AMPLIFIERS USI--ETC(U)
SEP 78 @ MON, H ROBINSON
HDL-TM-78-16

F/G 9/1

UNCLASSIFIED

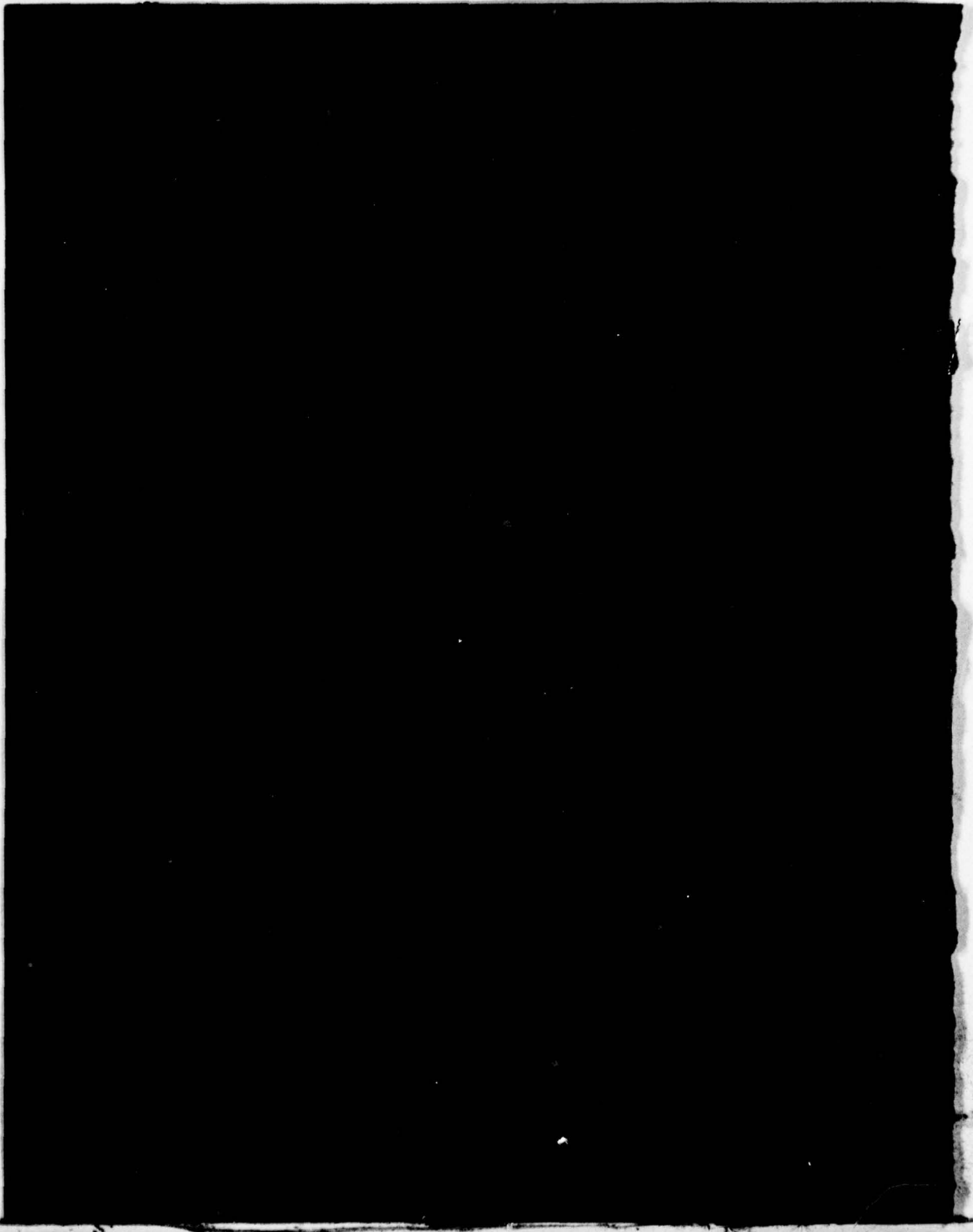
NL

| OF |
AD
A060756



AD A060756

DDC FILE COPY



51

UNCLASSIFIED

SECURITY CLASSIFICATION OF THIS PAGE(When Data Entered)

because the supply nozzle of the LPA has a large linear resistance component. Even without the supply nozzle linear component, the best that one can achieve is limited as indicated by the following equation:

$$Q_s = \frac{Q_T}{1 + \frac{K_s Q_s}{R_{bl}}}$$

where

Q_s = supply flow rate,

Q_T = total flow rate,

K_s = coefficient of the nonlinear component of the supply nozzle, and

R_{bl} = linear component of the bypass resistor.

The ideal ratio $\eta = (N_{Rf} - N_{Ri})_c / (N_{Rf} - N_{Ri})_u$ (where N_R is the Reynolds number, and the subscripts f, i, c, and u correspond to final, initial, compensated, and uncompensated) approaches 0.4 and 0.32 as Q_s/Q_T approaches zero for $\mu_f = 1/2 \mu_i$ and $\mu_f = 1/5 \mu_i$, respectively, where μ is dynamic viscosity.

In general, for a given viscosity range, the ratio η decreases as Q_s/Q_T decreases. Even though it is desirable to limit the variation in the Reynolds number over the military temperature range, we have to increase the total power supply to the system. Therefore, it is necessary to compromise between the value of the ratio η and the total supply flow to the compensated system.

ADDITIONAL TO	
DTIC	White Section <input checked="" type="checkbox"/>
DDI	Diff Section <input type="checkbox"/>
UNANNOUNCED	<input type="checkbox"/>
JUSTIFICATION	
SY	
DISTRIBUTION/AVAILABILITY CODES	
SPECIAL AVAIL. CODES/SPECIAL	
A	

DDC
RECEIVED
NOV 2 1978
RECEIVED
D

UNCLASSIFIED

2 SECURITY CLASSIFICATION OF THIS PAGE(When Data Entered)

CONTENTS

	<u>Page</u>
1. INTRODUCTION	5
2. THEORETICAL CONSIDERATIONS	5
3. LINEAR RESISTOR BYPASS FOR HYDRAULIC OPERATION	6
3.1 Analysis	8
3.2 Flow Resistance of LPA Supply Nozzle	9
3.3 Linear Bypass Resistor Design	12
4. EXPERIMENTAL TEST SETUP AND TEST RESULTS	15
4.1 Experimental Test Setup	15
4.2 Test Results and Theoretical Calculations	16
5. SUMMARY AND RECOMMENDATION	27
SYMBOLS	28
DISTRIBUTION	29

FIGURES

1 Schematic of laminar proportional amplifier	5
2 Pressure gain, G_p , versus temperature, T , and Reynolds number, N_R	6
3 Supply flow rate, Q_s , and Reynolds number, N_R , versus temperature T	7
4 Schematic of supply nozzle with bypass resistor	7
5 Schematic of supply nozzle of laminar proportional amplifier	10
6 Approximate presentation of the converging section of laminar proportional amplifier supply nozzle	11
7 Schematic of bypass resistor	12
8 Schematic of test setup	16
9 P-Q characteristics of laminar proportional amplifier supply nozzle	17
10 P-Q characteristics of two linear resistors in parallel	18
11 Pressure gain, G_p , versus Reynolds number	20

FIGURES (Cont'd)

	<u>Page</u>
12 Normalized pressure gain versus temperature at various constant flow rates	21
13 Normalized pressure gain versus temperature at various constant total flow rates	22
14 Comparison between the uncompensated and the compensated pressure gain versus temperature	23
15 Variation of the laminar proportional amplifier supply nozzle Reynolds number, N_R , versus temperature for various compensations.	24
16 Variation of the theoretical and experimental Reynolds number, N_R , versus temperature for the compensated laminar proportional amplifier	26
17 Ideal Reynolds number ratio; η versus Q_S/Q_T for the ideal laminar resistor bypass with $\mu_f = 1/2 \mu_i$ and $\mu_f = 1/5 \mu_i$	26
18 Variation of η versus μ_f/μ_i for various values of Q_T and c_d . .	27

1. INTRODUCTION

The purpose of this study is to extend the operating temperature range of the laminar proportional amplifier (LPA) (fig. 1) operating in hydraulic fluid by using a linear resistor bypass from the supply to the vent. This extension would allow the LPA to operate over a temperature range of 4.4 to 70 C. Within this temperature range, the kinematic viscosity of 5606 hydraulic oil changes from 40 to 7 centistoke, or about six times. This large change of viscosity presents a problem to the present LPA design because the LPA cannot operate satisfactorily over this temperature range because of variations in pressure gain, G_p , within the Reynolds number range. In order to maintain the pressure gain of the LPA within an acceptable level under these conditions, temperature compensation is needed. There are several ways to compensate the temperature effects; methods under consideration are linear resistor bypass, feedback, and power supply conditioning. This report deals only with the method of a linear resistor bypass. Test equipment limitations restricted the experimental temperature range to 15 to 55 C.

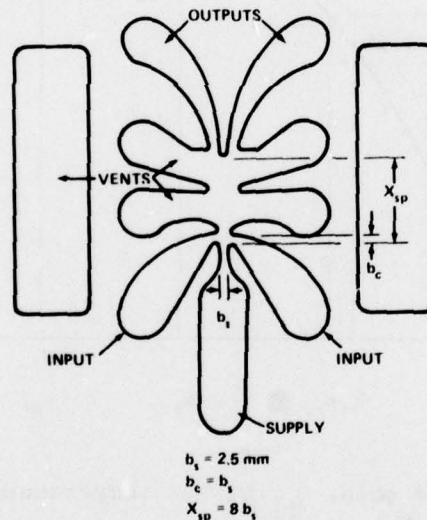


Figure 1. Schematic of laminar proportional amplifier.

2. THEORETICAL CONSIDERATIONS

The pressure gain of the LPA can be characterized by the Reynolds number $N_R = \bar{U}h/\nu$, based on average velocity, \bar{U} , channel height, h , and kinematic viscosity, ν . In general, G_p increases with N_R . At constant flow rate, the pressure gain increases as the hydraulic fluid temperature increases because N_R increases. Figure 2 illustrates the

problem. Assume that T_1 to T_4 is the desired temperature range. For this temperature range the pressure gain of a typical LPA varies from G_{p1} to G_{p4} , which is more than the desired gain variation of G_{p2} to G_{p3} . It is obvious that an acceptable solution to this problem is to have an LPA with a G_p versus N_R characteristic as shown by the dotted line in figure 2. At present, however, we do not have the desired LPA to meet the temperature requirement. In order to maintain the gain within G_{p2} to G_{p3} over the desired temperature range (T_1 to T_4), we have to temperature compensate the power supply so that the effective Reynolds number range is reduced to (N_{R2} to N_{R3}) from (N_{R1} to N_{R4}).

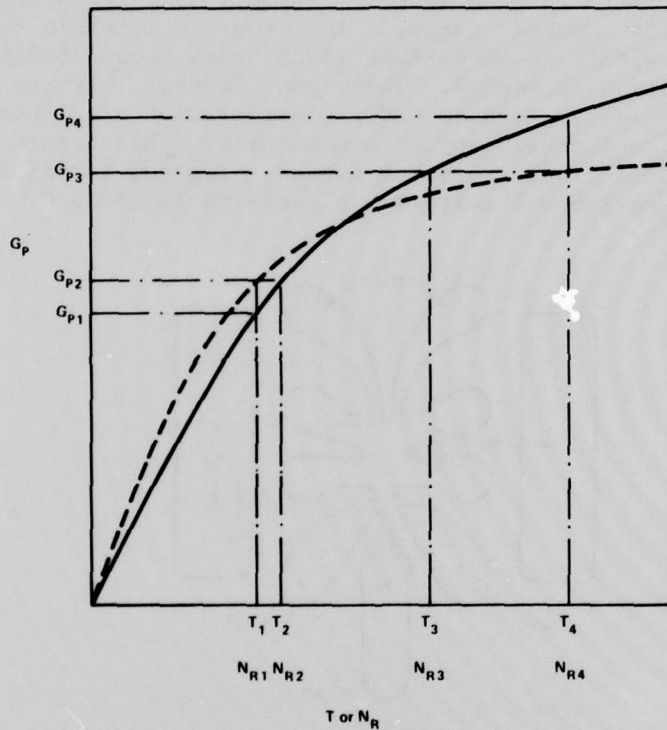


Figure 2. Pressure gain, G_p , versus temperature, T , and Reynolds number, N_R .

3. LINEAR RESISTOR BYPASS FOR HYDRAULIC OPERATION

In order to maintain the N_R through the LPA supply nozzle at a manageable range throughout the modified temperature range (4.4 to 70 C), we have to increase the supply flow rate, Q_s , as the fluid temperature decreases, and decrease the flow rate as the fluid temperature increases. Figure 3 shows the idealized compensation for

the flow rate to maintain the Reynolds number at a constant level regardless of the temperature changes. In other words, we have to maintain the ratio Q_s/ν at a constant level by scheduling the flow rate accordingly. One of the schemes for scheduling the flow rate is the use of a linear bypass resistor in parallel with the supply nozzle as shown in figure 4. The value of a linear resistor is proportional to the dynamic viscosity so that the flow through the resistor increases as the liquid temperature increases. As a result, for a constant total flow rate, flow through the LPA supply nozzle will decrease.

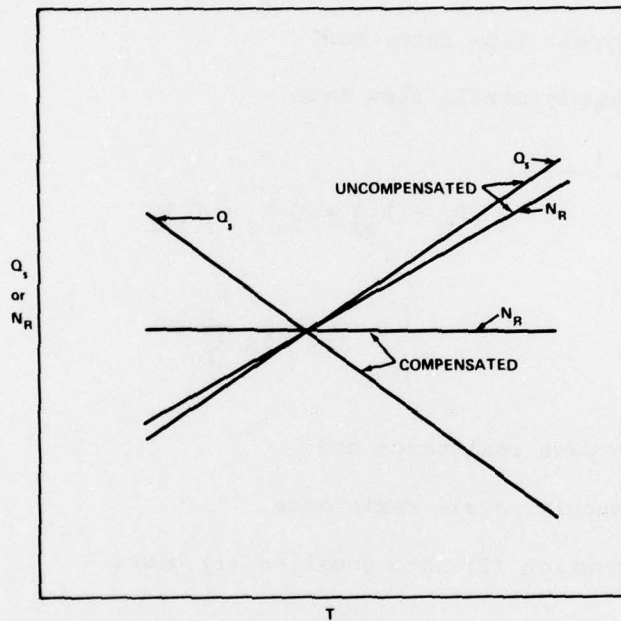


Figure 3. Supply flow rate, Q_s , and Reynolds number, N_R , versus temperature T .

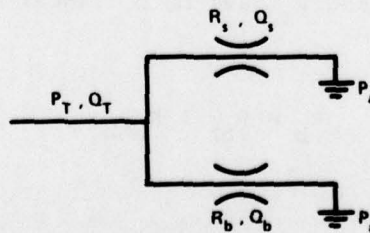


Figure 4. Schematic of supply nozzle with bypass resistor.

3.1 Analysis

From figure 4, we can write

$$Q_T = Q_s + Q_b , \quad (1)$$

where

Q_T = total flow rate,

Q_b = bypass flow rate, and

Q_s = supply nozzle flow rate.

Since

$$(P_T - P_a) = Q_s R_s = Q_b R_b ,$$

then

$$Q_b = Q_s \frac{R_s}{R_b} , \quad (2)$$

where

R_b = bypass resistance and

R_s = supply nozzle resistance.

Substituting equation (2) into equation (1) gives

$$Q_s = \frac{Q_T}{1 + \frac{R_s}{R_b}} . \quad (3)$$

In general R_b and R_s have both linear and nonlinear components such that

$$R_b = R_{bl} + K_b Q_b , \quad (4)$$

and

$$R_s = R_{sl} + K_s Q_s , \quad (5)$$

where

R_{bl} = linear component of the bypass resistor,

K_b = coefficient of the nonlinear component of the bypass resistor,

R_{sl} = linear component of the supply nozzle, and

K_s = coefficient of the nonlinear component of the supply nozzle.

Substituting equations (4) and (5) into equation (3) yields

$$Q_s = \frac{Q_T}{1 + \frac{R_{sl} + K_s Q_s}{R_{bl} + K_b Q_b}} \quad (6)$$

Equation (6) is the governing equation for the bypass system. In general, R_{sl} , R_{bl} , K_b , and K_s are functions of the fluid temperature. For hydraulic fluid within the desired temperature range, K_b and K_s can be assumed to be constant because the density, ρ , remains almost constant. The linear components, R_{bl} and R_{sl} , are, however, dependent on the fluid temperature because of viscosity changes due to temperature variations. The most effective compensation occurs when R_{sl} and K_b approach zero so that equation (6) becomes

$$Q_s = \frac{Q_T}{1 + \frac{K_s Q_s}{R_{bl}}} \quad (7)$$

Equation (7) describes the upper limit of the linear resistor bypass method.

In terms of Q_s , the Reynolds number is

$$N_R = Q_s / b_s \nu \quad (8)$$

3.2 Flow Resistance of LPA Supply Nozzle

The supply nozzle of the LPA can be represented by a rectangular channel with variable width as shown in figure 5.

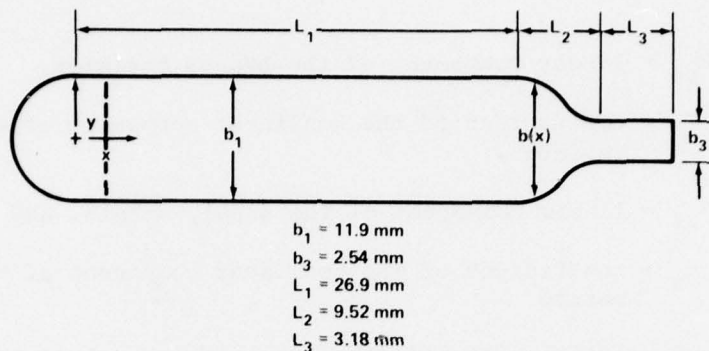


Figure 5. Schematic of supply nozzle of laminar proportional amplifier.

Bellman,¹ using Rouse's velocity profile, derives the resistance for a fully developed flow in a rectangular channel as

$$R = \frac{\mu L}{h^4 \left[\frac{\sigma}{12} + \frac{2}{\pi^5} \sum_{m=1}^{\infty} \frac{(1 - \cos m\pi)^2}{m^5} \frac{(-2e^{m\sigma\pi} - 2e^{-m\sigma\pi} + 4)}{e^{m\sigma\pi} - e^{-m\sigma\pi}} \right]}, \quad (9)$$

where

b = channel width,

h = channel depth,

L = length of the channel,

μ = dynamic viscosity, and

σ = local aspect ratio $\left(\sigma = \frac{h}{b} \right)$.

It should be noted that the resistance of fully developed channel flow is dependent only on the geometry and the dynamic viscosity of the fluid. Besides the linear component, we have to include the pressure drop due to flow development. Therefore, the total pressure drop, Δp , for a flow through a rectangular channel can be expressed as

¹R. H. Bellman, *Fluidic Proportional Amplifier for Very Low Reynolds Numbers*, *Fluidic State-of-the-Art Symposium*, Vol. 1, Harry Diamond Laboratories (1974).

$$\Delta p = \frac{\mu Q}{h^4} LD + K\rho \frac{Q^2}{A^2}, \quad (10)$$

where

K = flow development coefficient and

$$D = \frac{1}{\frac{\sigma}{12} + \frac{2}{\pi^5} \sum_{m=1}^{\infty} \frac{(1 - \cos m\pi)^2}{m^5} \left(\frac{-2e^{m\sigma\pi} - e^{-m\sigma\pi} + 4}{e^{m\sigma\pi} - e^{-m\sigma\pi}} \right)}. \quad (11)$$

In calculating the linear resistance in the converging section of the supply nozzle, we assume that the nozzle can be divided into small rectangular sections, as shown in figure 6, such that the total linear resistance can be calculated as

$$R_{l2} = \sum_{i=1}^n \frac{\mu}{h^4} (\Delta X_i D_i). \quad (12)$$

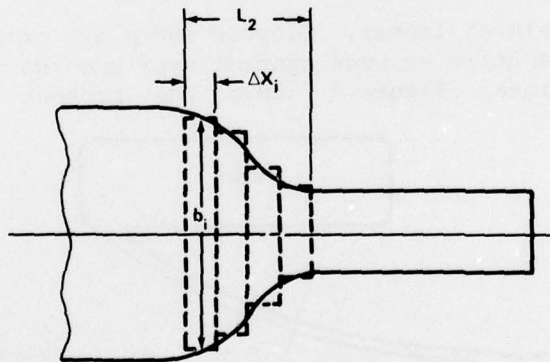


Figure 6. Approximate presentation of the converging section of laminar proportional amplifier supply nozzle.

In the supply nozzle (fig. 5), we also have to include the effect due to the converging section. Therefore, the total pressure drop for the supply nozzle can be written as

$$\Delta p_s = \frac{\mu Q_s}{h^4} \left(L_1 D_1 + \sum_{i=1}^n X_i D_i + L_3 D_3 \right) + \frac{K \rho Q_s^2}{(hb_1)^2} + \frac{1}{2} \left(\frac{\rho Q_s^2}{h^2} \right) \left[\left(\frac{1}{b_1^2} \right) - \left(\frac{1}{b_3^2} \right) \right], \quad (13)$$

and the total resistance can be written as

$$R_s = \frac{\Delta p_s}{Q_s} = \frac{\mu}{h^4} \left(L_1 D_1 + \sum_{i=1}^n \Delta X_i D_i + L_3 D_3 \right) + \frac{K \rho Q_s}{(hb_1)^2} + \frac{1}{2} \left(\frac{\rho Q_s}{h^2} \right) \left[\left(\frac{1}{b_1^2} \right) - \left(\frac{1}{b_3^2} \right) \right]. \quad (14)$$

It is assumed that the contribution due to developing flow in sections 2 and 3 can be neglected.

3.3 Linear Bypass Resistor Design

From equation (10), if

$$\frac{\mu L D}{h^4} \gg \frac{K \rho Q}{A^2}, \quad (15)$$

the resistor is almost linear. Since μ and ρ are properties of the fluid, the only parameters we have control over are the geometric parameters and the flow rate. Figure 7 shows the present design of the

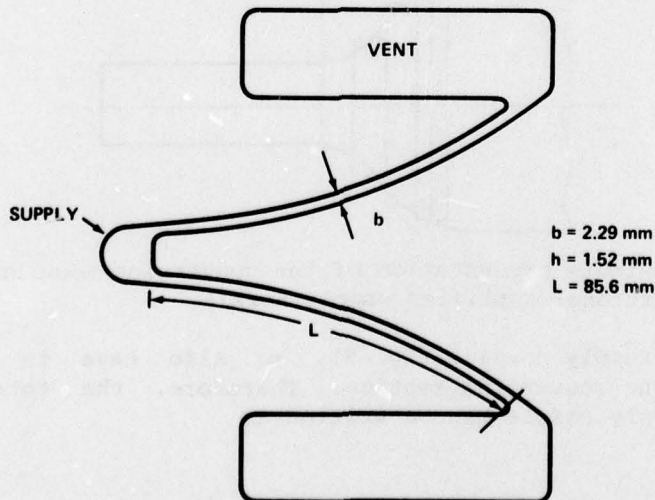


Figure 7. Schematic of bypass resistor.

linear bypass resistor. The design conforms to the LPA configuration so that the bypass resistor can be stacked in parallel with the LPA supply and venting manifolds to vary the resistance incrementally.

As mentioned earlier in section 3, the linear components, R_{sl} and R_{bl} , are dependent on the fluid temperature viscosity. From equation (10), we can write

$$R_s = R_{sl} + K_s Q_s, \quad (16)$$

where

$$R_{sl} = R_l \mu.$$

In order to simplify the calculation, let us normalize the following quantities at the operating point such that

$$R_s = R_l \mu + K_s Q_s = 1, \quad (17)$$

$$\mu = 1, \text{ and} \quad (18)$$

$$Q_s = 1. \quad (19)$$

Substituting equations (18) and (19) into (17) produces

$$R_l + K_s = 1 \text{ or} \quad (20)$$

$$R_l = 1 - K_s.$$

From the definition of the discharge coefficient, c_d , as given by Manion and Drzewiecki,² one can write

$$c_d = \left(\frac{K_s Q_s}{R_{sl} + K_s Q_s} \right)^{1/2}. \quad (21)$$

²F. Manion and T. Drzewiecki, *Analytical Design of Laminar Proportional Amplifier, Fluidic State-of-the-Art Symposium, Vol. 1, Harry Diamond Laboratories (1974).*

At the operating point, equation (22) becomes

$$c_d = \left(\frac{K_s}{R_1 + K_s} \right)^{1/2} \quad (22)$$

Substituting equation (20) into (22) and solving for K_s , we have

$$K_s = c_d^2 \quad (23)$$

and equation (20) becomes

$$R_1 = 1 - c_d^2 \quad (24)$$

Since the bypass resistor can be designed to have a very small nonlinear component, it is assumed that R_b is linear and can be written as

$$R_b = R'_b \mu \quad (25)$$

where R'_b is the geometric constant for the bypass resistor. With the above assumptions, equation (6) becomes

$$Q_s = \frac{-(R_1 + R'_b) + \left([(R_1 + R'_b)\mu]^2 + 4K_s Q_T R'_b \mu \right)^{1/2}}{2K_s} \quad (26)$$

With the aid of the assumption on normalization, one can show that

$$R'_b = \frac{1}{Q_T - 1} \quad (27)$$

In terms of μ , c_d , and Q_T , equation (26) becomes

$$Q_s = \frac{-\left(1 - c_d + \frac{1}{Q_T - 1}\right)\mu + \left\{ \left[\left(1 - c_d + \frac{1}{Q_T - 1}\right)\mu \right]^2 + 4Q_T c_d^2 \frac{\mu}{Q_T - 1} \right\}^{1/2}}{2c_d^2} \quad (28)$$

Equation (28) is the desired expression for Q_s as a function of μ , c_d , and Q_T . For an ideal nozzle, $c_d = 1$ and equation (28) becomes

$$Q_s = \frac{\mu}{1 - Q_T} + \frac{\left[\left(\frac{\mu}{Q_T - 1} \right)^2 + 4\mu \left(\frac{Q_T}{Q_T - 1} \right) \right]^{1/2}}{2} \quad (29)$$

The above equation describes the upper limits of the linear resistor bypass as a function of μ and Q_T .

The effectiveness of the linear resistor bypass can be shown by the ratio between the compensated and uncompensated Reynolds number ranges over the same temperature or viscosity range. This ratio can be written as

$$\eta = \frac{(N_{Rf} - N_{Ri})_c}{(N_{Rf} - N_{Ri})_u} \quad (30)$$

where N_{Ri} and N_{Rf} are the initial and final Reynolds numbers, respectively, and the subscripts c and u correspond to compensated and uncompensated. Since $(N_{Ri})_c = (N_{Ri})_u$, equation (30) can be written as

$$\eta = \frac{\left(\frac{N_{Rf}}{N_{Ri}} - 1 \right)_c}{\left(\frac{N_{Rf}}{N_{Ri}} - 1 \right)_u} \quad (31)$$

Equation (31) is the desired expression for the effectiveness of the linear resistor bypass.

4. EXPERIMENTAL TEST SETUP AND TEST RESULTS

4.1 Experimental Test Setup

In this study, a comprehensive experimental program was conducted to evaluate the flow shunting effectiveness of the linear resistor bypass. Figure 8 shows the schematic of the test setup. Dow Corning Silicone 200 fluid was chosen as the working fluid because its viscosity and density are very stable, and it is easier to handle than 5606 hydraulic oil. In this test the fluid temperature can be controlled between 15 and 55 C with an error of ± 0.25 C. All the

pressure measurements were made with Barocell pressure transducers, and the flow rates were measured with calibrated orifice flowmeters. In order to reduce the pump noise, an accumulator and an inline screen filter were placed model between the pump and the test section. The LPA tested was an HDL (3.1.1008C) with a 2.5-mm width supply nozzle.

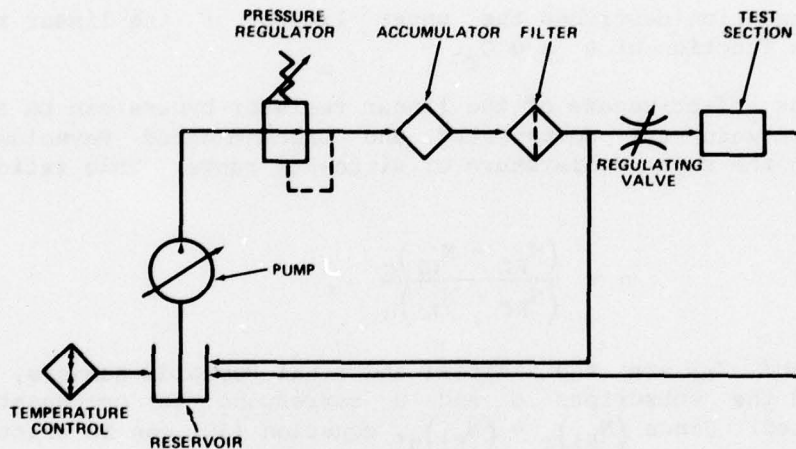


Figure 8. Schematic of test setup.

4.2 Test Results and Theoretical Calculations

In this test program, the pressure-flow (P-Q) characteristics of both the LPA supply nozzle and the resistor were measured at fluid temperatures of 15, 25, 35, 45, and 55 C. Figure 9 shows the experimental P-Q characteristics of the LPA as compared with the theoretical calculation using equation (14) for aspect ratios of 1.25, 2.5, and 5. The agreement is good. Similarly, figure 10 shows the P-Q characteristics for two, four, and eight linear resistors in parallel. Again the test results and the theoretical predictions are in good agreement. It should be noted that the value of the pressure drops has been multiplied by a constant, K_1 , to account for the pressure drop in the supply manifold. It should also be noted that both the test results and theoretical predictions indicate that the present resistor is "linear" within the test range.

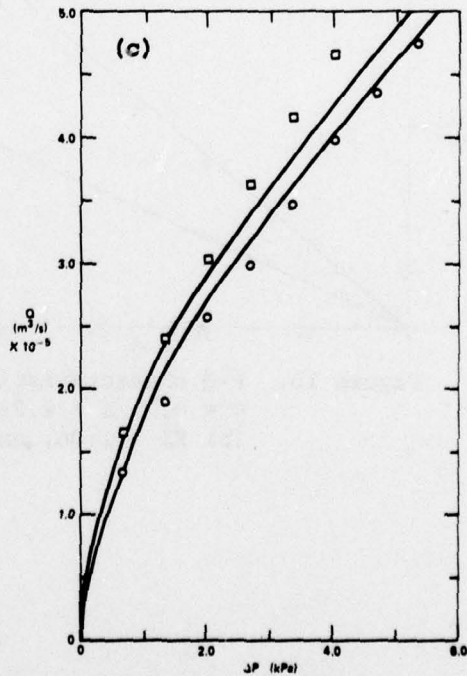
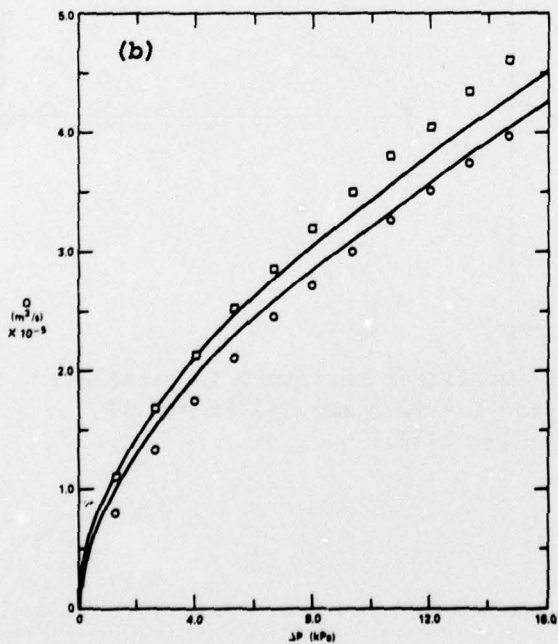
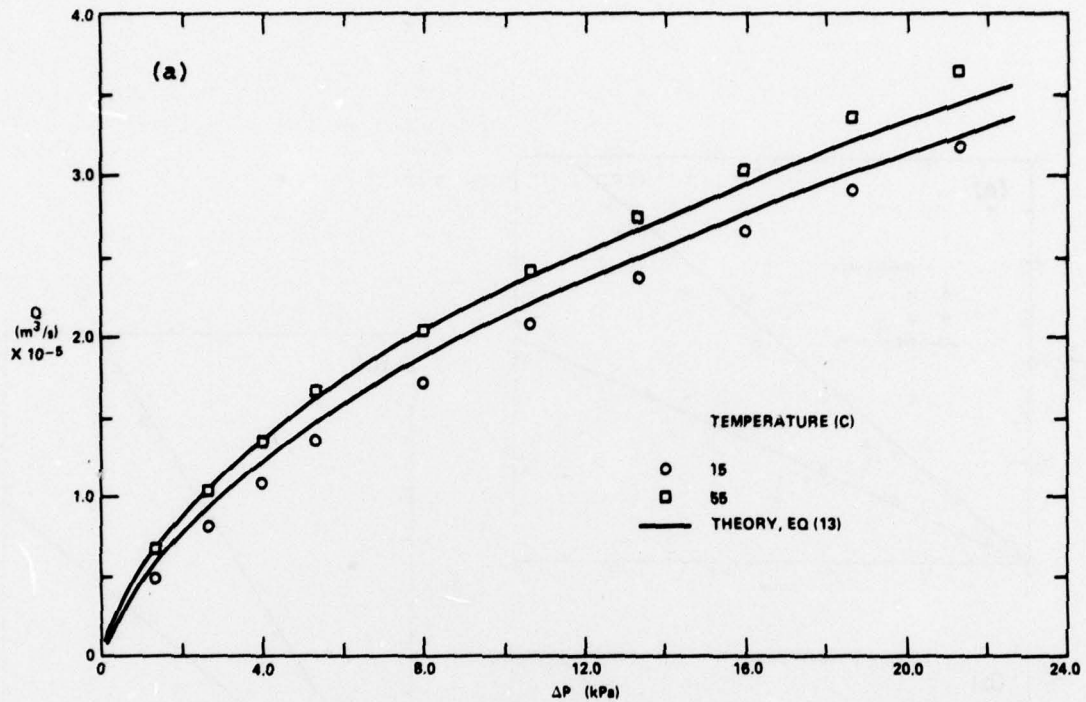


Figure 9. P-Q characteristics of laminar proportional amplifier supply nozzle; $K = 0.6$, and $b_s = 2.5$ mm; (a) $\sigma = 1.25$, (b) $\sigma = 5$, and (c) $\sigma = 2.5$.

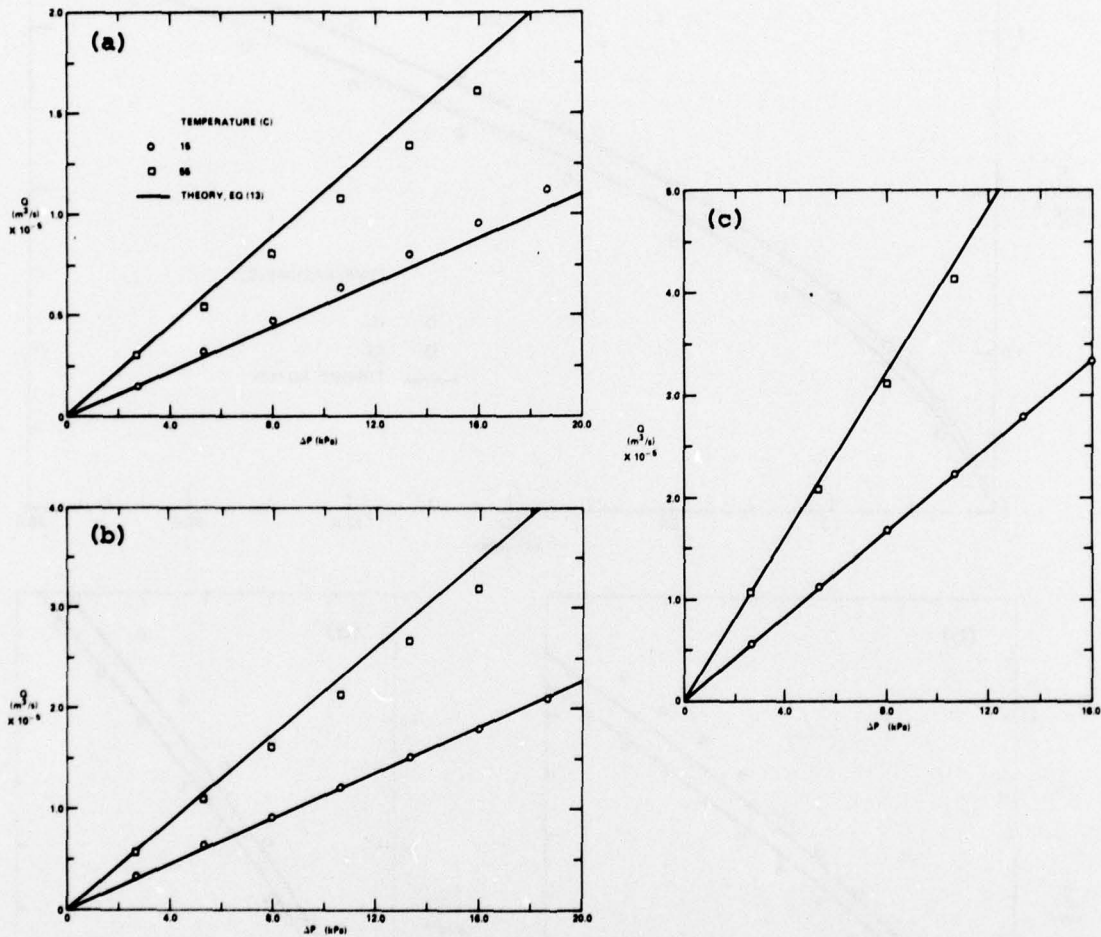


Figure 10. P-Q characteristics of two linear resistors in parallel; $\sigma = 0.7$, $b = 2.28$ mm, and $L = 82.5$ mm; (a) $K_1 = 1.02$, (b) $K_1 = 1.06$, and (c) $K_1 = 1.12$.

One of the most important performance characteristics of the LPA is the pressure gain. Figure 11 shows the blocked-load pressure gain, G_p , of the LPA versus the Reynolds number, $N_R = \bar{U}h/\nu$. In general, G_p increases as N_R increases. In order to evaluate the effectiveness of the linear resistor bypass on the pressure gain, the pressure gain was measured at various constant flow rates over the temperature range of 15 to 55 C. Figure 12 shows the normalized pressure gain versus temperature at various constant flow rates set at 25 C. Once again we see that G increases as the fluid temperature increases because the Reynolds number increases as the temperature increases for a constant flow rate. Figure 13 shows the normalized pressure gain versus temperature for various constant total flow rates for different combinations of the LPA and linear resistors.

In order to illustrate the effectiveness of linear resistor bypass, the uncompensated pressure gain characteristics are compared with several compensated gain characteristics in figure 14. Another way to measure the effectiveness of the linear resistor bypass is to compare the Reynolds number changes for the uncompensated, ideal compensated (eq (7)), and compensated (eq (6)) LPA over the same temperature range as shown in figure 15 for various combinations of LPA aspect ratios and bypass resistors. As indicated in these figures, for a given initial LPA supply nozzle Reynolds number, the ratio of the supply nozzle flow, Q_s , to the total flow, Q_T , determines the amount of compensation for the Reynolds number. An increase of the ratio Q_s/Q_T decreases the amount of compensation, while a decrease of Q_s/Q_T tends to increase the effectiveness of the compensation as shown in figures 15(g) and 15(c), respectively.

Figure 16 shows the predicted Reynolds number changes as compared with the experimental results. Figure 17 shows the theoretical limits of the Reynolds number ratio as a function of the Q_s/Q_T ratio for an ideal linear resistor bypass ($K_{bl}, R_{s1} = 0$) for $\mu_f = 1/2 \mu_1$ and $\mu_f = 1/5 \mu_1$. These limits were calculated by using equations (7) and (8) for various constant values of Q_T . Figure 18 shows the variations of η versus μ_f/μ_1 for various values of Q_T and c_d .

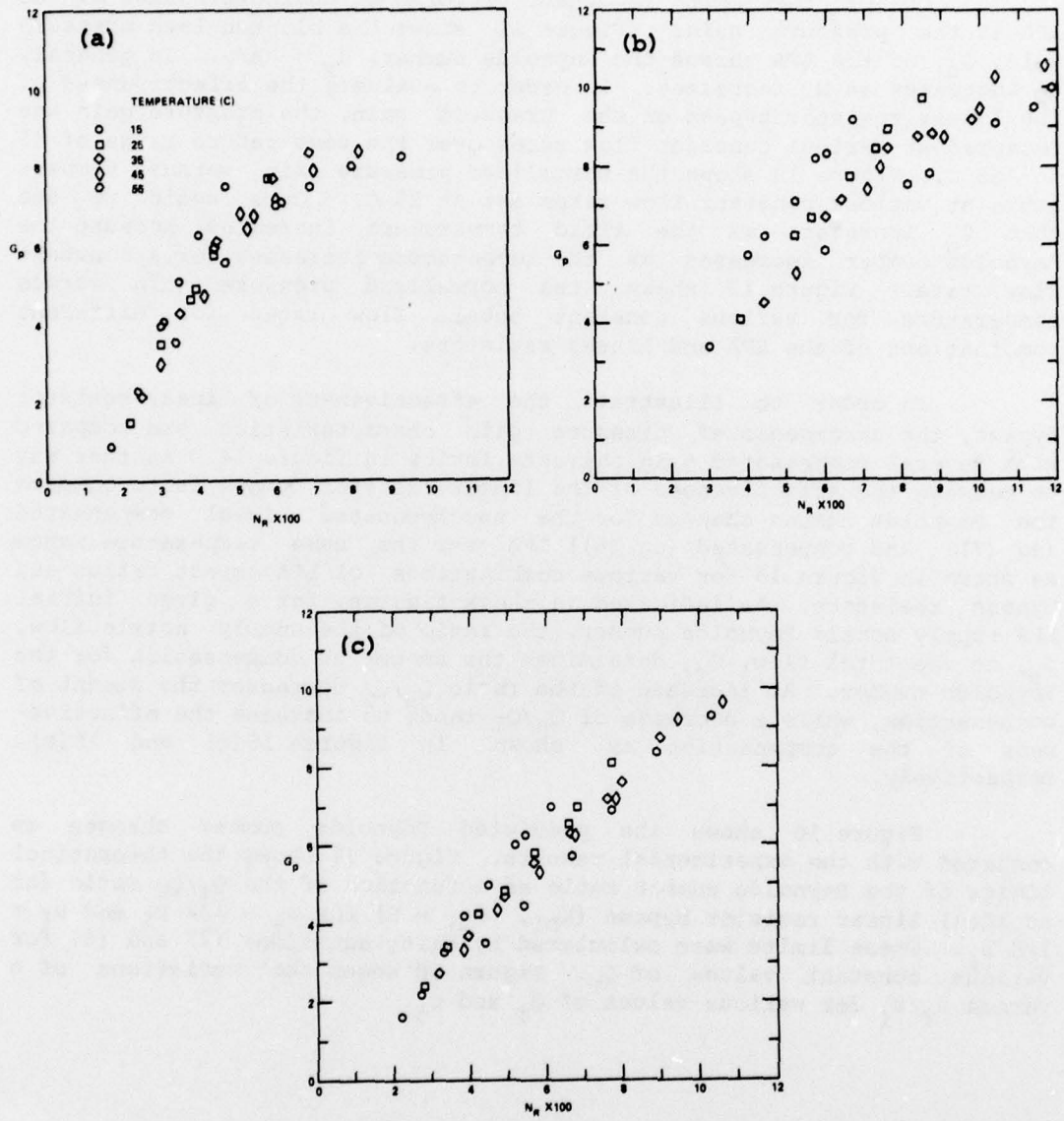


Figure 11. Pressure gain, G_p , versus Reynolds number, N_r ; (a) $\sigma = 1.25$, (b) $\sigma = 2.50$, and (c) $\sigma = 5.0$.

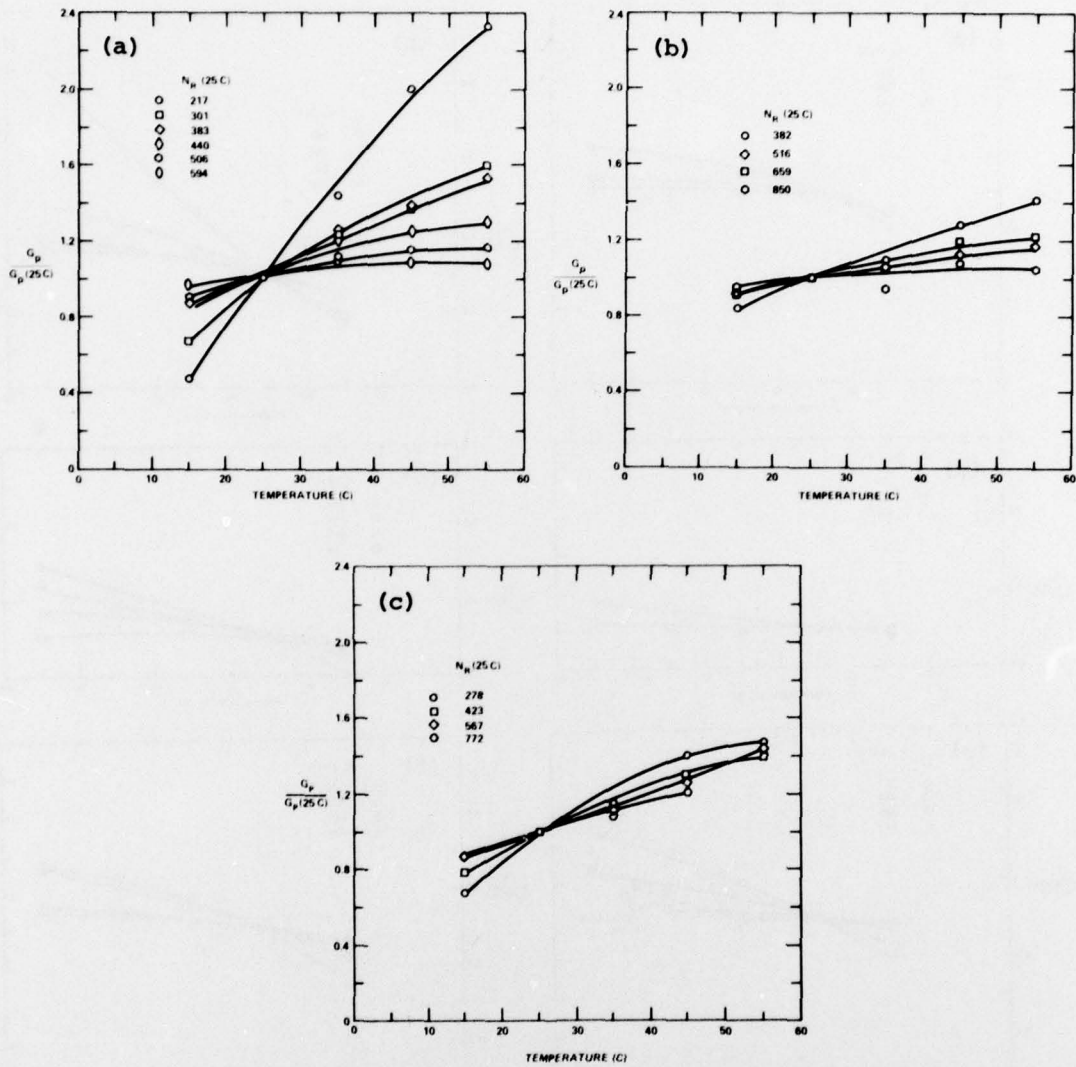


Figure 12. Normalized pressure gain versus temperature at various constant flow rates; (a) $\sigma = 1.25$, (b) $\sigma = 2.5$, and (c) $\sigma = 5.0$.

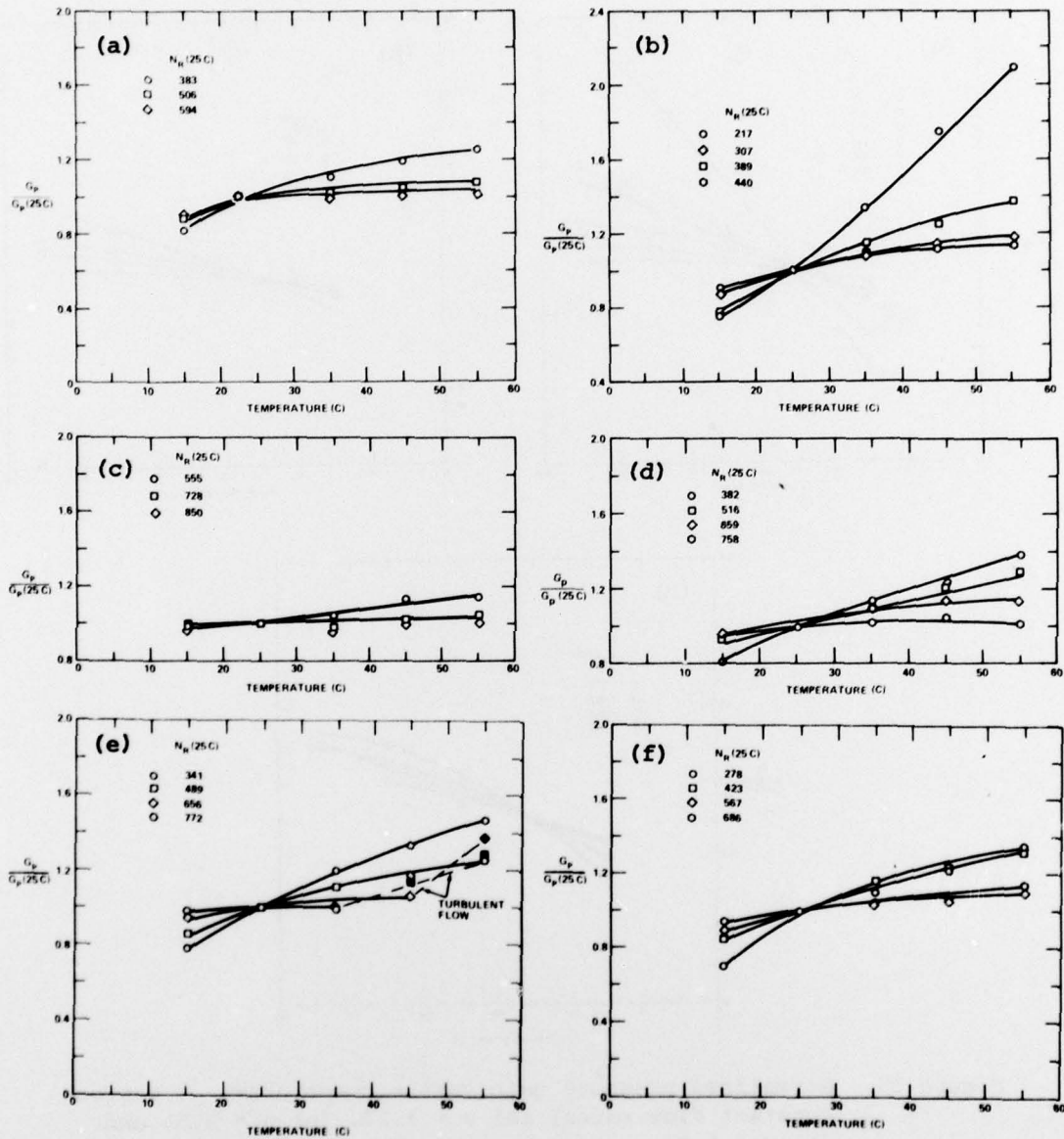


Figure 13. Normalized pressure gain versus temperature at various constant total flow rates; (a) $\sigma = 1.25$ and four resistors in parallel, (b) $\sigma = 1.25$ and eight resistors in parallel, (c) $\sigma = 2.5$ and four resistors in parallel, (d) $\sigma = 2.5$ and eight resistors in parallel, (e) $\sigma = 5.0$ and four resistors in parallel, and (f) $\sigma = 5.0$ and eight resistors in parallel.

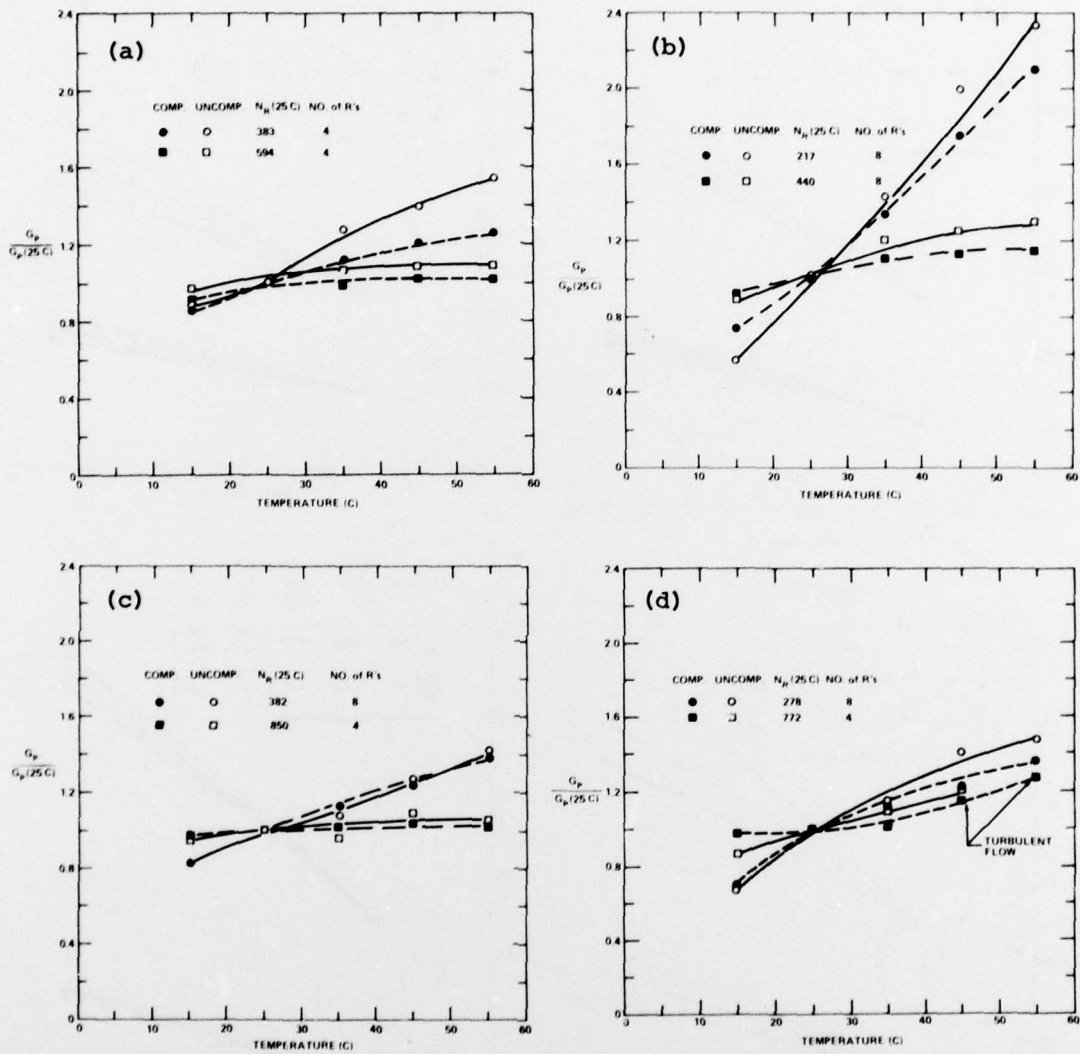


Figure 14. Comparison between the uncompensated and the compensated pressure gain versus temperature; (a) $\sigma = 1.25$ and four resistors in parallel, (b) $\sigma = 1.25$ and eight resistors in parallel, (c) $\sigma = 2.5$, and (d) $\sigma = 5.0$.

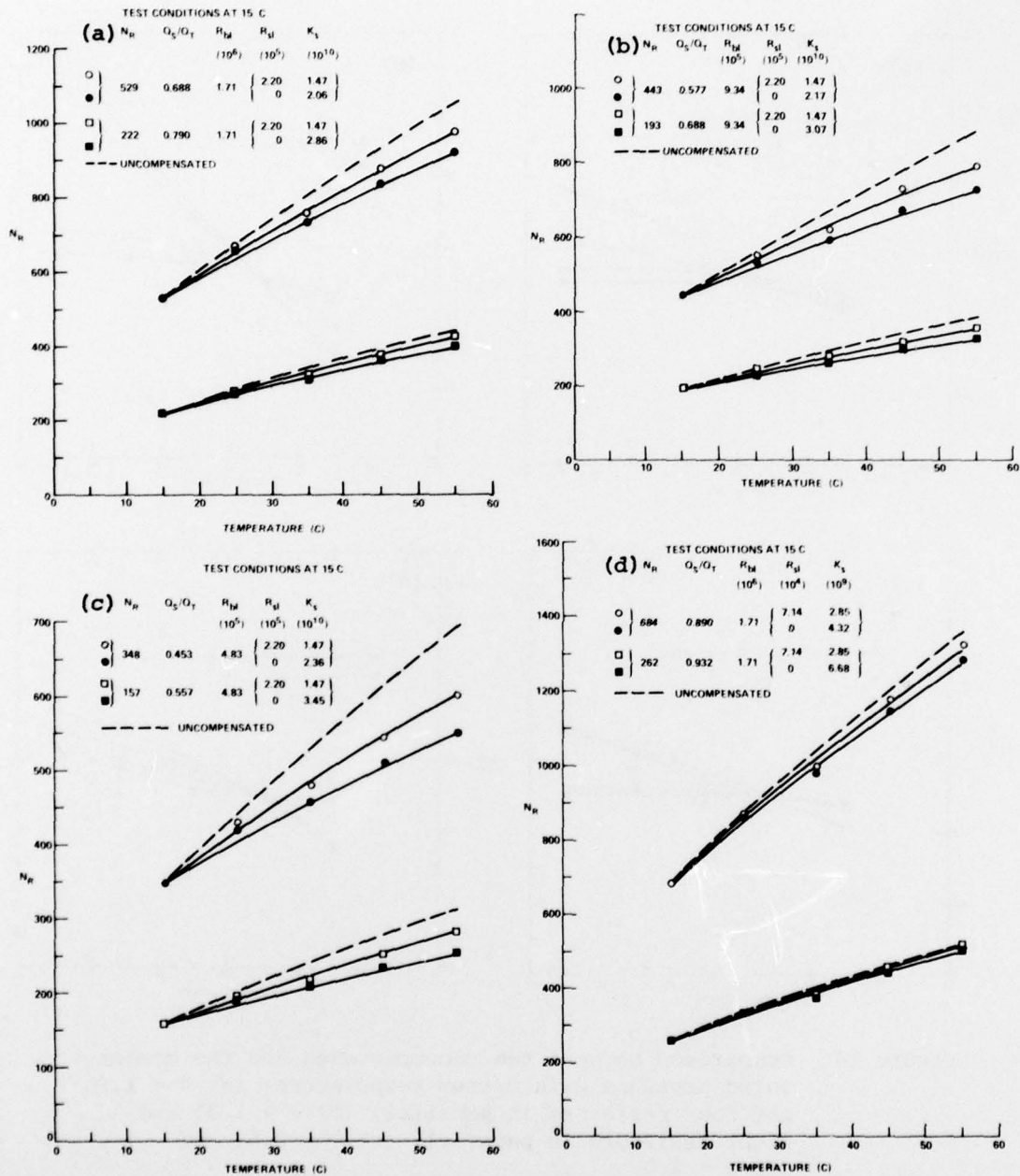


Figure 15. Variation of the laminar proportional amplifier supply nozzle Reynolds number, N_R , versus temperature for various compensations; (a) $\sigma = 1.25$, two resistors in parallel, (b) $\sigma = 1.25$, four resistors in parallel, (c) $\sigma = 1.25$, eight resistors in parallel, and (d) $\sigma = 2.50$, two resistors in parallel.

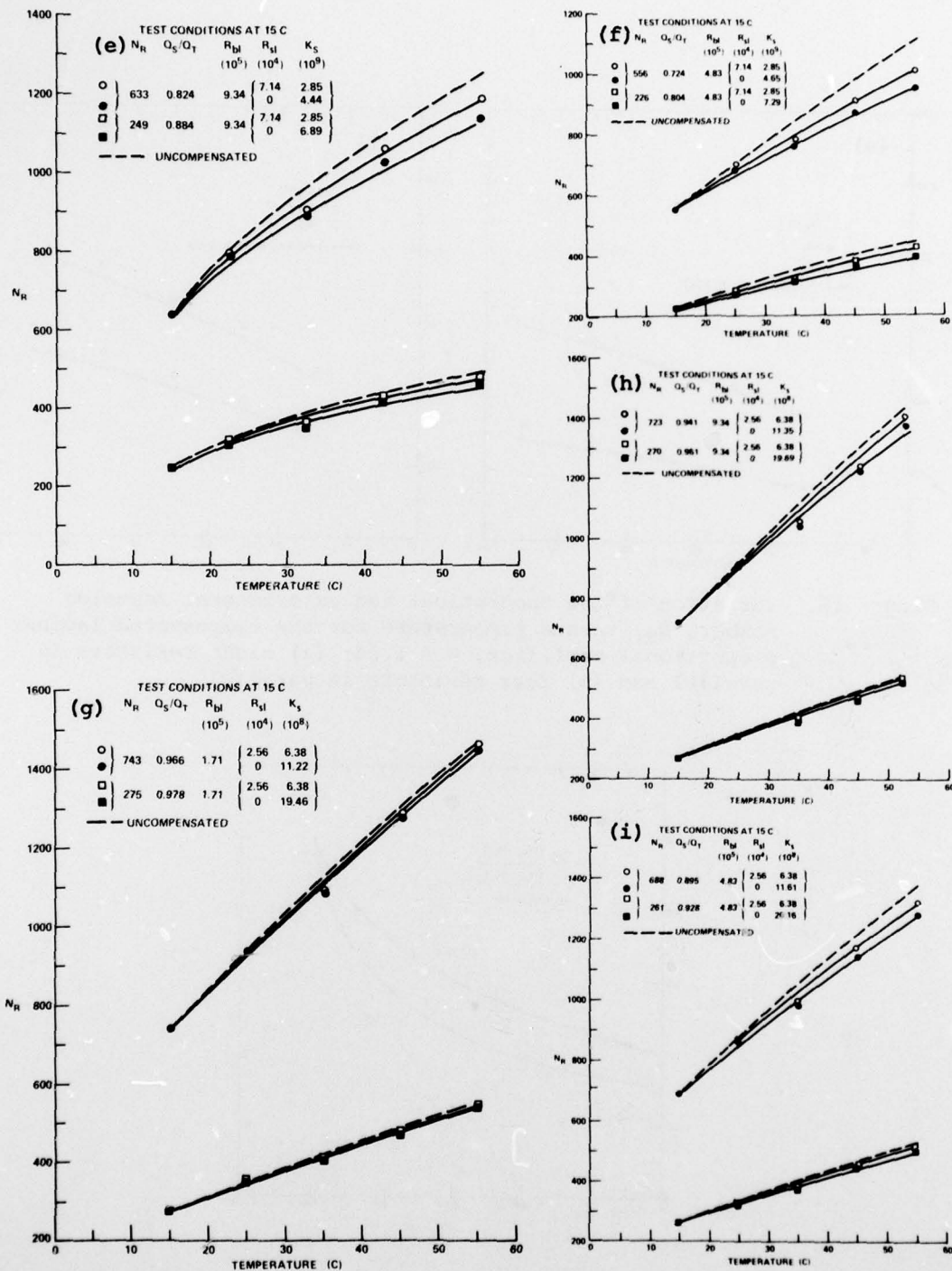


Figure 15. (e) $\sigma = 2.50$, four resistors in parallel, (f) $\sigma = 2.50$, eight resistors in parallel, (g) $\sigma = 5.0$, two resistors in parallel, (h) $\sigma = 5.0$, four resistors in parallel, and (i) $\sigma = 5.0$, eight resistors in parallel.

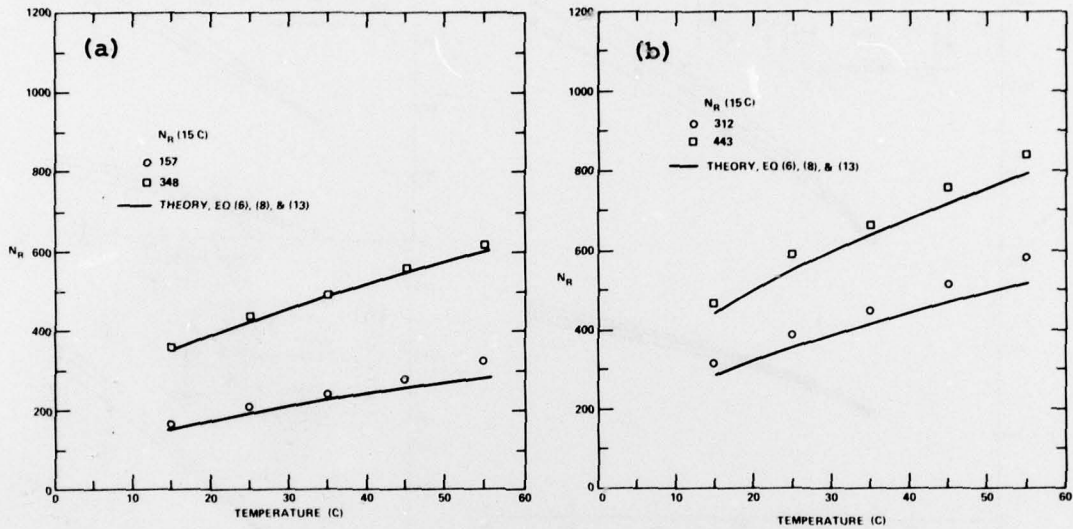


Figure 16. Variation of the theoretical and experimental Reynolds number, N_R , versus temperature for the compensated laminar proportional amplifier, $\sigma = 1.25$; (a) eight resistors in parallel and (b) four resistors in parallel.

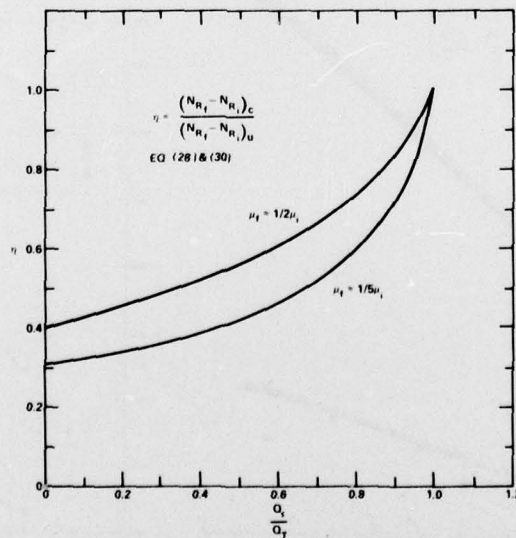


Figure 17. Ideal Reynolds number ratio; η versus Q_S/Q_T for the ideal linear resistor bypass with $\mu_f = 1/2 \mu_i$ and $\mu_f = 1/5 \mu_i$.

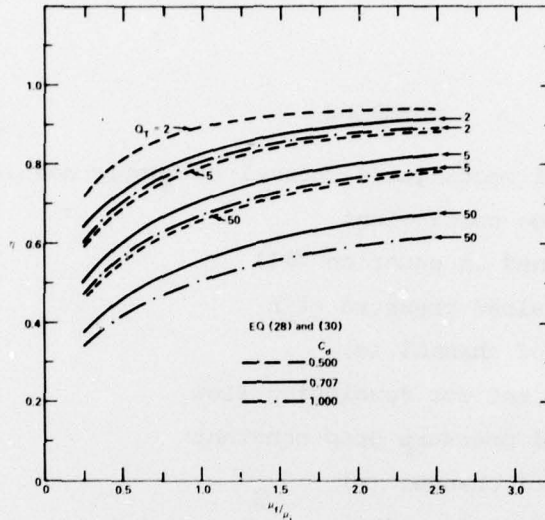


Figure 18. Variation of η versus μ_f/μ_i for various values of Q_s/Q_T and c_d .

5. SUMMARY AND RECOMMENDATION

A comprehensive experimental and theoretical study of the linear resistor bypass for the LPA supply has been conducted. In general the theoretical and the experimental results are in good agreement. The results of this study indicate that the use of a linear resistor bypass for temperature compensation in the present LPA design yields a limited success. The method is limited because the supply nozzle of the LPA has a large linear component as indicated both by the equations obtained by the least-squares fit of the data and the theoretical calculations. Even if we can design the LPA supply nozzle with a pure orifice, the effectiveness of the linear resistor bypass is still limited, as indicated by figure 17, which shows the upper limits of the linear resistor bypass as given by equation (7).

Both the theoretical and experimental results indicate that the effectiveness of the linear resistor bypass method is dependent on the ratio Q_s/Q_T and the linear resistance component of the LPA supply nozzle. This is illustrated clearly by the results shown in figures 15(c) and (g) for small and large values of Q_s/Q_T , respectively. Over the temperature range of 15 to 55 C, the Reynolds number change has been reduced by 30 percent for Q_s/Q_T equal to 0.453 while there is only a 2-percent reduction for Q_s/Q_T equal to 0.966. The above results also show that it is necessary to more than double the total flow in order to have a 30-percent reduction of the Reynolds number range for the temperature range of 15 to 55 C. Therefore a compromise is required between the amount of compensation and the total supply flow to the system.

In order to compensate the Reynolds number of the LPA over the military temperature range, other, more effective methods of temperature compensation should be investigated.

SYMBOLS

b	width of rectangular channel or supply nozzle (m)
c_d	discharge coefficient
D	as defined in equation (11)
G_p	blocked-load pressure gain
h	height of channel (m)
K	coefficient for developing flow
K _l	manifold pressure drop constant
L	length of channel (m)
N_R	$\bar{U}h/\nu$, Reynolds number
P	pressure (kN/m ²)
Q	flow rate (m ³ /s)
R	resistance (kg/m ⁴ -s)
T	temperature (C)
\bar{U}	average velocity (m/s)
X	length of channel or distance (m)
η	$(N_{Rf} - N_{Ri})_c (N_{Rf} - N_{Ri})_u$
μ	dynamic viscosity (kg/m-s)
ρ	density (kg/m ³)
σ	aspect ratio (h/b)
ν	kinematic viscosity (m ² /s)

Subscripts

1,2,...i index	m index
a ambient	n index
b bypass	s supply
c compensated	sp splitter
i index, initial	T total
f final	u uncompensated
l linear	

DISTRIBUTION

COMMANDER
US ARMY MATERIEL DEVELOPMENT &
READINESS COMMAND
5001 EISENHOWER AVENUE
ALEXANDRIA, VA 22333
ATTN DRXAM-TL, HQ TECH LIBRARY

COMMANDER
US ARMY MISSILE & MUNITIONS
CENTER & SCHOOL
REDSTONE ARSENAL, AL 35809
ATTN ATSK-CTD-F

DIRECTOR
US ARMY MATERIEL SYSTEMS
ANALYSIS ACTIVITY
ABERDEEN PROVING GROUND, MD 21005
ATTN DRXSY-MP

DIRECTOR
US ARMY BALLISTIC RESEARCH LABORATORY
ABERDEEN PROVING GROUND, MD 21005
ATTN DRDAR-TSB-S (STINFO)

COMMANDER IDDR&E
PENTAGON, ROOM 3D 1089
WASHINGTON, DC 20310
ATTN LTC G. KOPESAK

DEFENSE DOCUMENTATION CENTER
CAMERON STATION, BUILDING 5
ALEXANDRIA, VA 22314
ATTN DDC-TCA (12 COPIES)

OFFICE OF THE DEPUTY CHIEF OF STAFF FOR
RESEARCH, DEVELOPMENT & ACQUISITION
DEPARTMENT OF THE ARMY
WASHINGTON, DC 20310
ATTN DAMA-ARP-P, DR. V. GARBER
ATTN MR. JOHN HILL, ROOM 3D424

US ARMY R&D GROUP (EUROPE)
BOX 15
FPO NEW YORK 09510
ATTN CHIEF, AERONAUTICS BRANCH
ATTN CHIEF, ENGINEERING SCIENCES

US ARMY RESEARCH OFFICE
P. O. BOX 12211
RESEARCH TRIANGLE PARK, NC 27709
ATTN JAMES J. MURRAY, ENG SCI DIV

BMD ADVANCED TECHNOLOGY CENTER
P.O. BOX 1500
HUNTSVILLE, AL 35807
ATTN J. PAPADOPOULOS

COMMANDER
USA FOREIGN SCIENCE & TECHNOLOGY CENTER
FEDERAL OFFICE BUILDING
220 7th STREET, NE
CHARLOTTESVILLE, VA 22901
ATTN DRXST-SD1

DIRECTOR
APPLIED TECHNOLOGY LABORATORY
FORT EUSTIS, VA 23604
ATTN GEORGE W. FOSDICK, DAVDL-EU-SYA

COMMANDER
USA MISSILE RES & DEV COMMAND
REDSTONE ARSENAL, AL 35809
ATTN REDSTONE SCIENTIFIC INFORMATION
CENTER, DRSMI-RBD
ATTN DRDMI-TGC, WILLIAM GRIFFITH
ATTN DRDMI-TGC, J. C. DUNAWAY
ATTN DRCPM-TOE, FRED J. CHEPLEN

COMMANDER
USA MOBILITY EQUIPMENT R&D CENTER
FORT BELVOIR, VA 22060
ATTN TECHNICAL LIBRARY (VAULT)
ATTN DRDME-EM, R. N. WARE

COMMANDER
EDGEWOOD ARSENAL
ABERDEEN PROVING GROUND, MD 21010
ATTN SAREA-MT-T, MR. D. PATTON

COMMANDER
US ARMY ARRADCOM
DOVER, NJ 07801
ATTN SARPA-TS-S-#59
ATTN DRDAR-LCN-F, A. E. SCHMIDLIN
ATTN DRDAR-LCW-E, MR. J. CONNOR

COMMANDER
WATERVLIET ARSENAL
WATERVLIET ARSENAL, NY 12189
ATTN SARWV-RDT-L

COMMANDER
USA TANK AUTOMOTIVE RES & DEV COMMAND
ARMOR & COMP DIV, DRDTA-RKT
BLDG 215
WARREN, MI 48090
ATTN T. KOZOWYK
ATTN M. STEELE

COMMANDER
WHITE SANDS MISSILE RANGE, NM 88002
ATTN STEWS-AL-L, TECHNICAL LIBRARY

DISTRIBUTION (Cont'd)

COMMANDER
US ARMY ARMAMENT MATERIEL READINESS
COMMAND
ROCK ISLAND, IL
ATTN DRSAR-RDG-T, MR. R. SPENCER
ATTN DRSAR-ASF

OFFICE OF NAVAL RESEARCH
DEPARTMENT OF THE NAVY
ARLINGTON, VA 22217
ATTN STANLEY W. DOROFF, CODE 438
ATTN D. S. SIEGEL, CODE 211

DEPARTMENT OF THE NAVY
R&D PLANS DIVISION
ROOM 5D760, PENTAGON
WASHINGTON, DC 20350
ATTN BENJ R. PETRIE, JR.
OP-987P4

COMMANDER
NAVAL AIR DEVELOPMENT CENTER
WARMINSTER, PA 18974
ATTN R. MCGIBONEY, 30424
ATTN CODE 8134, LOIS GUISE

NAVAL AIR SYSTEMS COMMAND
DEPARTMENT OF THE NAVY
WASHINGTON, DC 20360
ATTN CODE AIR-52022A, J. BURNS
ATTN CODE AIR-52022E, D. HOUCK

COMMANDER
PACIFIC MISSILE RANGE
NAVAL MISSILE CENTER
POINT MUGU, CA 93042
ATTN CODE 3123, ABE J. GARRETT
ATTN CODE 1243, A. ANDERSON

COMMANDER
NAVAL SHIP ENGINEERING CENTER
PHILADELPHIA DIVISION
PHILADELPHIA, PA 19112
ATTN CODE 6772, D. KEYSER

COMMANDER
NAVAL SURFACE WEAPONS CENTER
WHITE OAK, MD 20910
ATTN CODE 413, CLAYTON MCKINDRA
ATTN CODE WA-33, J. O'STEEN

COMMANDER
NAVAL ORDNANCE STATION
INDIANHEAD, MD 20640
ATTN CODE 5123B, J. MORRIS

NAVAL SHIP RES & DEV CENTER
CODE 1619, MR. K. READER
BETHESDA, MD 20084

NAVAL SEA SYSTEMS COMMAND
SEA0331H
WASHINGTON, DC 20362
ATTN A. CHAIKIN

COMMANDER
NAVAL WEAPONS CENTER
CHINA LAKE, CA 93555
ATTN CODE 533, LIBRARY DIVISION
ATTN CODE 5536, MR. M. D. JACOBSON

COMMANDER
AF AERO PROPULSION LABORATORY, AFSC
WRIGHT-PATTERSON AFB, OH 45433
ATTN LESTER SMALL 1TBC

COMMANDER
AIR FORCE AVIONICS LABORATORY
WRIGHT-PATTERSON AFB, OH 45433
ATTN RWN-2, RICHARD JACOBS

DIRECTOR
AF OFFICE OF SCIENTIFIC RESEARCH
1400 WILSON BLVD
ARLINGTON, VA 22209
ATTN NE, MR. GEORGE KNAUSENBERGER

COMMANDER
AIR FORCE FLIGHT DYNAMICS LABORATORY
WRIGHT-PATTERSON AFB, OH 45433
ATTN AFFDL/FGL, H. SNOWBALL

COMMANDER
AF WEAPONS LABORATORY, AFSC
KIRTLAND AFB, NM 87117
ATTN SUL, TECHNICAL LIBRARY

COMMANDER
ARMAMENT DEVELOPMENT AND TEST CENTER
EGLIN AIR FORCE BASE, FL 32542
ATTN ADTC (DLOSL), TECH LIBRARY

AIR FORCE FLIGHT TEST CENTER
6510 ABG/SSD
EDWARDS AFB, CA 93523
ATTN TECHNICAL LIBRARY

AF INSTITUTE OF TECHNOLOGY, AU
WRIGHT-PATTERSON AFB, OH 45433
ATTN LIBRARY AFIT(LD),
BLDG 640, AREA B
ATTN AFIT(ENM), MILTON E. FRANKE

AEROSPACE MEDICAL DIVISION
BROOKS AFB, TX 78235
ATTN AMD/RDN, CPT G. JAMES

DIV. OF REACTOR RES & DEV
F-309 USERDA
WASHINGTON, DC 20545
ATTN FRANK C. LEGLER

DISTRIBUTION (Cont'd)

OAK RIDGE NATIONAL LABORATORY
CENTRAL RES LIBRARY, BLDG 4500N, RM 175
P. O. BOX X
OAK RIDGE, TN 37830
ATTN E. HOWARD

DEPT OF HEW
PUBLIC HEALTH SERVICE
NATIONAL INSTITUTE OF HEALTH
BLDG 13, RM 3W-13
BETHESDA, MD 20014
ATTN C. J. MCCARTHY

DEPARTMENT OF COMMERCE
BUREAU OF EAST-WEST TRADE
OFFICE OF EXPORT ADMINISTRATION
WASHINGTON, DC 20230
ATTN WALTER J. RUSNACK

SCIENTIFIC LIBRARY
US PATENT OFFICE
WASHINGTON, DC 20231
ATTN MRS. CURETON

DEPARTMENT OF COMMERCE
NATIONAL BUREAU OF STANDARDS
WASHINGTON, DC 20234
ATTN GUSTAVE SHAPIRO, 425.00

NASA AMES RESEARCH CENTER
MOFFETT FIELD, CA 94035
ATTN MS 244-13, DEAN CHISEL

NASA LANGLEY RESEARCH CENTER
HAMPTON, VA 23665
ATTN MS 494, H. D. GARNER
ATTN MS 494, R. R. HELLBAUM
ATTN MS 185, TECHNICAL LIBRARY

NASA LEWIS RESEARCH CENTER
21000 BROOKPARK ROAD
CLEVELAND, OH 44135
ATTN VERNON D. GEBBEN

NASA SCIENTIFIC & TECH INFO FACILITY
P. O. BOX 8657
BALTIMORE/WASHINGTON INTERNATIONAL
AIRPORT, MD 21240
ATTN ACQUISITIONS BRANCH

UNIVERSITY OF ALABAMA
CIVIL & MINERAL ENGINEERING DEPT.
P. O. BOX 1468
UNIVERSITY, AL 35486
ATTN DR. HAROLD R. HENRY

ARIZONA STATE UNIVERSITY
ENGINEERING CENTER
TEMPE, AZ 85281
ATTN PETER K. STEIN, LABORATORY
FOR MEASUREMENT SYSTEMS ENGR.

UNIVERSITY OF ARKANSAS
TECHNOLOGY CAMPUS
P. O. BOX 3017
LITTLE ROCK, AR 72203
ATTN PAUL C. MCLEOD

UNIVERSITY OF ARKANSAS
MECHANICAL ENGINEERING
FAYETTEVILLE, AR 72701
ATTN JACK H. COLE, ASSOC PROF

CARNEGIE-MELLON UNIVERSITY
SCHENLEY PARK
PITTSBURGH, PA 15213
ATTN PROF W. T. ROULEAU,
MECH ENGR DEPT

CASE WESTERN RESERVE UNIVERSITY
UNIVERSITY CIRCLE
CLEVELAND, OH 44106
ATTN PROF P. A. ORNER

THE CITY COLLEGE OF THE CITY
UNIVERSITY OF NY
DEPT OF MECH ENGR
139th ST. AT CONVENT AVE
NEW YORK, NY 10031
ATTN PROF L. JIJI
ATTN PROF G. LOWEN

DUKE UNIVERSITY
COLLEGE OF ENGINEERING
DURHAM, NC 27706
ATTN C. M. HARMAN

ENGINEERING SOCIETIES LIBRARY
345 EAST 47TH STREET
NEW YORK, NY 10017
ATTN HOWARD GORDON

FRANKLIN INSTITUTE OF THE STATE
OF PENNSYLVANIA
20TH STREET & PARKWAY
PHILADELPHIA, PA 19103
ATTN KA-CHEUNG TSUI, ELEC ENGR DIV
ATTN C. A. BELSTERLING

IIT RESEARCH INSTITUTE
10 WEST 35th STREET
CHICAGO, IL 60616
ATTN DR. K. E. MCKEE

LEHIGH UNIVERSITY
DEPARTMENT OF MECHANICAL ENGINEERING
BETHLEHEM, PA 18015
ATTN PROF FORBES T. BROWN

LINDA HALL LIBRARY
5109 CHERRY STREET
KANSAS CITY, MO 64110
ATTN DOCUMENTS DIVISION

DISTRIBUTION (Cont'd)

MASSACHUSETTS INSTITUTE OF TECHNOLOGY
77 MASSACHUSETTS AVENUE
CAMBRIDGE, MA 02139

ATTN ENGINEERING TECHNICAL REPORTS,
RM 10-408
ATTN DAVID WORMLEY, MECH ENGR DEPT,
RM 3-146

MICHIGAN TECHNOLOGICAL UNIVERSITY
LIBRARY, DOCUMENTS DIVISION
HOUGHTON, MI 49931
ATTN J. HAWTHORNE

UNIVERSITY OF MISSISSIPPI
201 CARRIER HALL, DEPT OF MECH ENGR
UNIVERSITY, MS 38677
ATTN DR. JOHN A. FOX

MISSISSIPPI STATE UNIVERSITY
DRAWER ME
STATE COLLEGE, MS 39672
ATTN DR. C. J. BELL, MECH ENG DEPT

UNIVERSITY OF NEBRASKA LIBRARIES
ACQUISITIONS DEPT, SERIALS SECTION
LINCOLN, NE 68508
ATTN ALAN GOULD

UNIVERSITY OF NEW HAMPSHIRE
MECH ENGR DEPT, KINGSBURY HALL
DURHAM, NH 03824
ATTN PROF CHARLES TATE

DEPARTMENT OF MECHANICAL ENGINEERING
NEWARK COLLEGE OF ENGINEERING
323 HIGH STREET
NEWARK, NJ 07102
ATTN DR. R. Y. CHEN

OHIO STATE UNIVERSITY LIBRARIES
SERIAL DIVISION, MAIN LIBRARY
1858 NEIL AVENUE
COLUMBUS, OH 43210

OKLAHOMA STATE UNIVERSITY
SCHOOL OF MECH & AEROSPACE ENGR.
STILLWATER, OK 74074
ATTN PROF KARL N. REID

MIAMI UNIVERSITY
DEPT OF ENG TECH
SCHOOL OF APPLIED SCIENCE
OXFORD, OH 45056
ATTN PROF S. B. FRIEDMAN

PENNSYLVANIA STATE UNIVERSITY
215 MECHANICAL ENGINEERING BUILDING
UNIVERSITY PARK, PA 16802
ATTN DR. J. L. SHEARER

PENNSYLVANIA STATE UNIVERSITY
ENGINEERING LIBRARY
201 HAMMOND BLDG
UNIVERSITY PARK, PA 16802
ATTN M. BENNETT, ENGINEERING LIBRARIAN

PURDUE UNIVERSITY
SCHOOL OF MECHANICAL ENGINEERING
LAFAYETTE, IN 47907
ATTN PROF. VICTOR W. GOLDSCHMIDT
ATTN PROF. ALAN T. MCDONALD

ROCK VALLEY COLLEGE
3301 NORTH MULFORD ROAD
ROCKFORD, IL 61101
ATTN KEN BARTON

RUTGERS UNIVERSITY
LIBRARY OF SCIENCE & MEDICINE
NEW BRUNSWICK, NJ 08903
ATTN GOVERNMENT DOCUMENTS DEPT
MS. SANDRA R. LIVINGSTON

SYRACUSE UNIVERSITY
DEPT OF MECH & AEROSPACE ENGINEERING
139 E. A. LINK HALL
SYRACUSE, NY 13210
ATTN PROFESSOR D. S. DOSANJH

UNIVERSITY OF TEXAS AT AUSTIN
DEPT OF MECHANICAL ENGINEERING
AUSTIN, TX 78712
ATTN DR. A. J. HEALEY

THE UNIVERSITY OF TEXAS AT ARLINGTON
MECHANICAL ENGINEERING DEPARTMENT
ARLINGTON, TX 76019
ATTN DR. ROBERT L. WOODS

TULANE UNIVERSITY
DEPT OF MECHANICAL ENGINEERING
NEW ORLEANS, LA 70118
ATTN H. F. HRUBECKY

UNION COLLEGE
MECHANICAL ENGINEERING
SCHENECTADY, NY 12308
ATTN ASSOC PROF W. C. AUBREY
MECH ENGR DEPT, STEINMETZ HALL

VIRGINIA POLYTECHNIC
INSTITUTE OF STATE UNIV
MECHANICAL ENGINEERING DEPARTMENT
BLACKSBURG, VA 24061
ATTN PROF H. MOSES

WASHINGTON UNIVERSITY
SCHOOL OF ENGINEERING
P. O. BOX 1185
ST. LOUIS, MO 63130
ATTN W. M. SWANSON

DISTRIBUTION (Cont'd)

WEST VIRGINIA UNIVERSITY
MECHANICAL ENGINEERING DEPARTMENT
MORGANTOWN, WV 26505
ATTN DR. RICHARD A. BAJURA

WICHITA STATE UNIVERSITY
WICHITA, KS 67208
ATTN DEPT AERO ENGR, E. J. RODGERS

UNIVERSITY OF WISCONSIN
MECHANICAL ENGINEERING DEPARTMENT
1513 UNIVERSITY AVENUE
MADISON, WI 53706
ATTN FEDERAL REPORTS CENTER
ATTN NORMAN H. BEACHLEY, DIR,
DESIGN ENGINEERING LABORATORIES

WORCESTER POLYTECHNIC INSTITUTE
WORCESTER, MA 01609
ATTN GEORGE C. GORDON LIBRARY (TR)
ATTN TECHNICAL REPORTS

AIRESEARCH
P. O. BOX 5217
402 SOUTH 36th STREET
PHOENIX, AZ 85034
ATTN DAVID SCHAFFER
ATTN TREVOR SUTTON
ATTN TOM TIPPETTS

AVCO SYSTEMS DIVISION
201 LOWELL STREET
WILMINGTON, MA 01887
ATTN W. K. CLARK

BELL HELICOPTER COMPANY
P. O. BOX 482
FORTWORTH, TX 76101
ATTN MR. R. D. YEARY

BENDIX CORPORATION
ELECTRODYNAMICS DIVISION
11600 SHERMAN WAY
N. HOLLYWOOD, CA 90605
ATTN MR. D. COOPER

BENDIX CORPORATION
RESEARCH LABORATORIES DIV.
BENDIX CENTER
SOUTHFIELD, MI 48075
ATTN C. J. AHERN

BOEING COMPANY, THE
P. O. BOX 3707
SEATTLE, WA 98124
ATTN HENRIK STRAUB

BOWLES FLUIDICS CORPORATION
9347 FRASER AVENUE
SILVER SPRING, MD 20910
ATTN VICE PRES./ENGR.

DR. RONALD BOWLES
2105 SONDRAL COURT
SILVER SPRING, MD 20904

CONTINENTAL CAN COMPANY
TECH CENTER
1350 W. 76TH STREET
CHICAGO, IL 60620
ATTN P. A. BAUER

CORDIS CORPORATION
P. O. BOX 428
MIAMI, FL 33137
ATTN STEPHEN F. VADAS, K-2

CORNING GLASS WORKS
FLUIDIC PRODUCTS
HOUGHTON PARK, B-2
CORNING, NY 14830
ATTN MR. W. SCHEMERHORN

CHRYSLER CORPORATION
P.O. BOX 118
CIMS-418-33-22
DETROIT, MI 48231
ATTN MR. L. GAU

EMX ENGINEERING, INC
BOX 216 - 216 LITTLE FALLS RD
CEDAR GROVE, NJ 07009
ATTN ANTHONY P. CORRADO, PRESIDENT

FLUIDICS QUARTERLY
P. O. BOX 2989
STANFORD, CA 94305
ATTN D. H. TARUMOTO

GENERAL ELECTRIC COMPANY
SPACE/RES DIVISIONS
P. O. BOX 8555
PHILADELPHIA, PA 19101
ATTN MGR LIBRARIES, LARRY CHASEN

GENERAL MOTORS CORPORATION
DELCO ELECTRONICS DIV
MANFRED G. WRIGHT
NEW COMMERCIAL PRODUCTS
P. O. BOX 1104
KOKOMO, IN 46901
ATTN R. E. SPARKS

GRUMMAN AEROSPACE CORPORATION
TECHNICAL INFORMATION CENTER
SOUTH OYSTER BAY ROAD
BETHPAGE, L. I., NY 11714
ATTN C. W. TURNER, DOCUMENTS
LIBRARIAN

HONEYWELL, INC.
1625 ZARTHAN AVE
MINNEAPOLIS, MI 55413
ATTN J. HEDEEN

DISTRIBUTION (Cont'd)

JOHNSON CONTROLS, INC
507 E. MICHIGAN
MILWAUKEE, WI 53201
ATTN WARREN A. LEDERMAN

MOORE PRODUCTS COMPANY
SPRING HOUSE, PA 19477
ATTN MR. R. ADAMS

MARTIN MARIETTA CORPORATION
AEROSPACE DIVISION
P. O. BOX 5837
ORLANDO, FL 32805
ATTN R. K. BRODERSON, MP 326
ATTN VITO O. BRAVO, MP 326

NATIONAL FLUID POWER ASSOCIATION
3333 NORTH MAYFAIR ROAD
MILWAUKEE, WI 53222
ATTN JOHN R. LUEKE
DIR OF TECH SERVICES

RICHARD WHITE & ASSOCIATES
ELECTRO/MECHANICAL ENGINEERS
77 PELHAM ISLE ROAD
SUDBURY, MA 01776
ATTN RICHARD P. WHITE

ROCKWELL INTERNATIONAL CORPORATION
COLUMBUS AIRCRAFT DIVISION,
P. O. BOX 1259
4300 E. 5TH AVENUE
COLUMBUS, OH 43216
ATTN MR. MARVIN SCHWEIGER

SANDIA CORPORATION
KIRTLAND AFB, EAST
ALBUQUERQUE, NM 87115
ATTN WILLIAM R. LEUENBERGER, DIV 2323

TRITEC, INC
P.O. BOX 56
COLUMBIA, MD 21045
ATTN L. SIERACKI

UNITED TECHNOLOGIES RESEARCH CENTER
400 MAIN STREET
E. HARTFORD, CT 06108
ATTN R. E. OLSON, MGR FLUID
DYNAMICS LABORATORY

US ARMY ELECTRONICS RESEARCH
& DEVELOPMENT COMMAND
ATTN WISEMAN, ROBERT S., DR., DRDEL-CT
ATTN PAO

HARRY DIAMOND LABORATORIES
ATTN 00100, COMMANDER/TECHNICAL DIR/TSO
ATTN CHIEF, 00210
ATTN CHIEF, DIV 10000
ATTN CHIEF, DIV 20000
ATTN CHIEF, DIV 30000
ATTN CHIEF, DIV 40000
ATTN CHIEF, LAB 11000
ATTN CHIEF, LAB 13000
ATTN CHIEF, LAB 15000
ATTN CHIEF, LAB 22000
ATTN CHIEF, LAB 21000
ATTN CHIEF, LAB 34000
ATTN CHIEF, LAB 36000
ATTN CHIEF, LAB 47000
ATTN CHIEF, LAB 48000
ATTN RECORD COPY, 94100
ATTN HDL LIBRARY, 41000 (5 COPIES)
ATTN HDL LIBRARY, 41000 (WOODBRIDGE)
ATTN CHAIRMAN, EDITORIAL COMMITTEE
ATTN TECHNICAL REPORTS BRANCH, 41300
ATTN LEGAL OFFICE, 97000
ATTN LANHAM, C., 00210
ATTN WILLIS, B., 47400
ATTN CHIEF, 13400 (10 COPIES)
ATTN DRZEWIECKI, T., 13400
ATTN MON, G., 13400 (10 COPIES)